Development 128, 4229-4239 (2001)
Printed in Great Britain © The Company of Biologists Limited 2001
DEV7904

rst and its paralogue *kirre* act redundantly during embryonic muscle development in *Drosophila*

Martin Strünkelnberg[1,*], Bernhard Bonengel[1,*], Livia M. Moda[2], Alexander Hertenstein[1], H. Gert de Couet[1,3], Ricardo G. P. Ramos[2] and Karl-Friedrich Fischbach[1,‡]

[1]Institut für Biologie III, Schänzlestr.1, Albert-Ludwigs-Universität, D-79104 Freiburg im Breisgau, Germany
[2]Departmento de Biologia Celular, Molecular e Bioagentes Patogênicos, Faculdade de Medicina de Ribeirão Preto, Universidade de São Paulo, Av. Bandeirantes 3900, 14.049-900 Ribeirão Preto-SP, Brazil
[3]Department of Zoology, University of Hawaii at Manoa, 2538 McCarthy Mall, Honolulu, HI 96822, USA
*These two authors contributed equally to this work
‡Author for correspondence (e-mail: kff@uni-freiburg.de)

Accepted 25 July 2001

SUMMARY

The polynucleate myotubes of vertebrates and invertebrates form by fusion of myoblasts. We report the involvement of the *Drosophila melanogaster* Roughest (Rst) protein as a new membrane-spanning component in this process. Rst is strongly expressed in mesodermal tissues during embryogenesis, but *rst* null mutants display only subtle embryonic phenotypes. Evidence is presented that this is due to functional redundancy between Rst and its paralogue Kirre. Both are highly related single-pass transmembrane proteins with five extracellular immunoglobulin domains and three conserved motifs in the intracellular domain. The expression patterns of *kirre* and *rst* overlap during embryonic development in muscle founder cells. Simultaneous deletion of both genes causes an almost complete failure of fusion between muscle founder cells and fusion-competent myoblasts. This defect can be rescued by one copy of either gene. Moreover, Rst, like Kirre is a myoblast attractant.

Key words: *Drosophila*, *kirre*, *duf*, *rst*, *irreC*, Fusion-competent myoblast, Muscle founder cell, Myoblast fusion

INTRODUCTION

The larval abdominal body wall musculature of *Drosophila* consists of a regular, repetitive array of 30 different muscles per hemisegment. Each muscle has a unique morphology, orientation and position (Bate, 1990; Bate, 1993), and consists of one single polynucleate myotube, while vertebrate muscles consist of bundles of several myotubes. Common to both, the myotubes are formed by fusion of mesodermal cells (Baylies et al., 1998). Therefore, *Drosophila* is a well suited model organism in which to study the genetics of myoblast fusion.

Specification of the muscle pattern starts during early embryonic development. After formation of the mesodermal cell layer, the mesoderm becomes subdivided into different cell types based on levels of *twist* expression: low levels mark future visceral and heart mesoderm, high levels prospective somatic mesoderm (Baylies and Bate, 1996).

In the prospective somatic mesoderm, four cell groups are specified dorsally, dorsolaterally, ventrolaterally and ventrally by the expression of *lethal of scute*. From each of these groups, one muscle progenitor cell is singled out by lateral inhibition (Carmena et al., 1995). These cells divide asymmetrically and provide the embryo with a subpopulation of myoblasts, the muscle founder cells. The expression of genes such as *S59* and *krüppel*, which specifically affect subsets of muscles, is already switched on in corresponding founder cell subsets. Therefore, the unique character of each future muscle is already 'programmed' into individual founder cells (Frasch, 1999).

The syncytial myotubes form during stages 11-14, when the founder cells fuse with myoblasts of a second class, the fusion-competent myoblasts. These cells do not contribute to the identity of an individual muscles, but rather provide cell material for the outgrowing muscle (Bate, 1990; Rushton et al., 1995).

Based on mutational analysis, several steps in the myoblast fusion process can be distinguished (Paululat et al., 1999): attraction and adhesion of fusion-competent myoblasts to founder cells (blocked in *mbc*, *sns* and *Df(1)w^{67k30}* mutants (Rushton et al., 1995; Bour et al., 2000; Ruiz-Gomez et al., 2000); alignment of fusion-competent myoblasts and founder cells with paired vesicles on either side of the adjoining membranes (the prefusion complex); the formation of electron-dense plaques; and, finally, vesiculation and membrane breakdown.

For attraction, binding and the initiation of fusion, fusion-competent myoblasts and founder cells need an asymmetric equipment of extracellular membrane-bound components that allows for attraction and discrimination; fusion-competent myoblasts and founder cells fuse only with cells from the other group, rather than with themselves (Baylies et al., 1998).

Recently, two genes encoding members of the immunoglobulin superfamily, *sns* and *kirre* (*kirre* was also named *dumbfounded*; Ruiz-Gomez et al., 2000), have been reported to show the expected features. Both encode transmembrane cell adhesion molecules involved in myoblast attraction and/or fusion. While Sns is expressed only on fusion-competent myoblasts, but not on founder cells (Bour et al., 2000), *kirre* is expressed selectively in the latter, but not in fusion-competent myoblasts. We present new data concerning the role of *kirre* and the involvement of its paralogue *rst* (Ramos et al., 1993; Reiter et al., 1996) in myoblast fusion.

MATERIALS AND METHODS

Fly stocks and genetic methods

All stocks used in this work have been previously described. Maintenance and manipulation of *Drosophila* stocks was performed at 25°C on standard-cornmeal-molasses-agar food. Staging of embryos was performed according to Campos-Ortega and Hartenstein (Campos-Ortega and Hartenstein, 1997).

For misexpression and rescue experiments, we used $Df(1)w^{67k30}$, $N^{fa\text{-}g}$ (courtesy of S. Artavanis-Tsakonas). The cross for the rescue was $Df(1)w^{67k30}$, $N^{fa\text{-}g}$*/FM7;+/+;UAS-rst/+* × *FM7/Y;twi-Gal4/+;twi-Gal4/+*. Lack of epidermal Rst expression was used as a marker for the $Df(1)w^{67k30}$ chromosome, and remnants of ectopic Rst in the midgut region served as a marker for *UAS-rst* driven by *twi-Gal4*.

Cloning of the *kirre* cDNA

During isolation of the *D. virilis* orthologue of *rst* (M. S., unpublished) we serendipitously isolated a related, paralogous sequence. We subsequently identified and cloned the corresponding *D. melanogaster* sequence, which we named *kirre*, using RT-PCR based on data of the EDGP (*Cosmid 163A10* – Accession Number, AL035436; Benos et al., 2000). The complete *kirre* cDNA sequence is available in GenBank under the Accession Number AF196553.

RT-PCR

Using the primers 5′-AGCACACCGCTTGAATCAGA-3′ and 5′-ACAGATGCAGCACAGCACTTA-3′ specific for sequences upstream from the two possible adenylation sites of the annotated *kirre* open reading frame (Benos et al., 2000), we performed reverse transcription (Superscript II, Life Industries) of 5 μg of total *D. melanogaster* pupal RNA followed by a RNase H (Life Industries) digestion as described by the manufacturer. Using *Pfu* turbo DNA-polymerase (Stratagene), 10 μl of the resulting cDNA was used in a 100 μl PCR with 60 pmol of primers that flank the complete *kirre* ORF (5′-TTAAACATGAGTGGCCAGAGG-3′ and 5′-TTGCCGC-TGAAAATGAAGCG-3′). PCR conditions were 94°C for 3 minutes, 35 cycles of 94°C for 1 minute, 55°C for 1 minute and 72°C for 12 minutes, and finally 15 minutes at 72°C. PCR was performed in a Robocycler (Stratagene).

The untranslated regions (UTRs) were cloned using the Rapid Amplification of cDNA ends (RACE) protocol as described elsewhere (Dieffenbach and Dveksler, 1995). For the 3′UTR, the adapter primer $CCAGTGAGCAGAGTGACGAT_{15}$ was used in RT of 5 μg of total pupal RNA as above. Primers for PCR were 5′-CAGAGTCCG-TCCGGTCAGTT-3′ and 5′-CCAGTGAGCAGAGTGACG-3′, and in a nested PCR 5′-GACCTCTGGCCACTCATGTT-3′ and 5′-GAGG-ACTCGAGCTCAAGC-3′.

For the 5′-UTR, the primer 5′-GGCGGAACGAGAACGGTTAG-3′ was used in RT of 0.5 μg commercial embryonal polyA-RNA (Clontech) as above. Nested PCRs were performed using 5′-GC-GGATAAATGTCCAATGAG-3′ and 5′-TGCCGACCATCGAGTAG-CGT-3′ with adapter primers as above. Amplification products were subcloned into the pCRII-TOPO vector (Invitrogen) and sequenced until all ambiguities were resolved.

Single fly PCR

One to three flies of the relevant genotype were frozen in liquid nitrogen and incubated overnight at –80°C. After addition of 50 μl 1× PCR buffer per fly, the mixture was heated to 94°C for 3 minutes and tissue was mechanically disrupted. The resulting solution (5 μl) was used in a standard 50 μl PCR reaction. Primers specific for *kirre* were 5′-CTGATCCTGACGCTGCTCCT-3′ and 5′-GGCGGAACGAGAA-CGGTTAG-3′. Primers spanning the presumed transcriptional start site of *rst* were 5′-CACTCTGACTAATTCACAATG-3′ and 5′-GAGTTGAGATCAAAGAGCCCAG-3′. PCR conditions were: 94°C for 3 minutes, 5 cycles of 94°C for 1 minute, 58°C for 2 minutes and 72°C for 40 seconds, and then 30 cycles of 94°C for 30 seconds, 56°C for 40 seconds and 72°C for 40 seconds, followed by 72°C for 10 minutes.

In-situ hybridization

Embryo dechorionation, devitellination and fixation was carried out as previously described (Ashburner, 1989). In situ hybridization was performed as described previously (Oxtoby and Jowett, 1993) and, for probe [K], according to Tautz and Pfeifle (Tautz and Pfeifle, 1989). Probes were selected on the basis of least nucleotide sequence similarity to exclude potential cross-hybridization. For *kirre* two different probes were used with identical results: probe [K] was isolated using the primers 5′-CAAGAGCGAACAGAGCAAGA-3′ and 5′-CATCTGAACATCGGGCATCG-3′. Probe [K intra] was isolated using the primers 5′-GTAATACCGGAGGCATCACG-3′ and 5′-TTAAACATGAGTGGCCAGAGG-3′. As for *rst*, we used a probe isolated using the primers 5′CTGTAAGAAGCGCACCAAGC3′ and 5′-GCTAAGTGCCTAACCTAAGC-3′.

Immunocytochemistry and microscopy

Immunocytochemistry was performed as described (Schneider et al., 1995). Antibodies used were against myosin heavy chain (1:1000-1:10,000; Kiehart and Feghali, 1986), Rst (1:10, mAB24A5.1; Schneider et al., 1995), β-3-tubulin (1:1000, provided by R. Renkawitz-Pohl), β-galactosidase (1:1000, abcam, Cambridge, UK) and GFP (1:250, abcam). Laser scanning microscopy was carried out with Leica TCS-NT and Leica TCS4D microscopes. Data were processed using AMIRA-2.2 (Indeed, Berlin, Germany) and Photoshop (Adobe).

Heat shock treatment

Homozygous *pCa18ZΔ3.1* flies (Moda et al., 2000) were placed on grape juice plates for 1 hour to lay eggs. Eggs were allowed to develop at 25°C for 7 hours and then incubated in a waterbath at 34.5°C for 4 hours. This means that individual embryos were heat-shocked starting at late stage 11 to late stage 12 until late stage 14 to mid stage 15. Controls were treated at 25°C instead of 34.5°C.

RESULTS

Overexpression of *rst* interferes with muscle development

Although the embryonic *rst* expression pattern is highly dynamic, none of the known loss-of-function mutations is lethal (Ramos et al., 1993). We used *pCa18ZΔ3.1* flies (Moda et al., 2000) to overexpress a secretable extracellular version of the protein by heat shock induction. Heat shocks applied during stages 12 to 15 induced embryonic lethality. Analysis of these embryos revealed muscle defects (Fig. 1A-D). Secretable Rst interfered with myoblast fusion. In heat shocked *pCa18ZΔ3.1* embryos, the muscles were thinner and more

unfused myoblasts could be observed than in heatshocked *yw* control embryos.

Additionally, we used the UAS/Gal4 system (Brand and Perrimon, 1993) to express a full-length *rst*-construct under transcriptional control of the *da-Gal4* driver (Wodarz et al., 1995). The genotype *da-Gal4/+;UAS-rst/+*, caused embryonic lethality and induced defects in myoblast fusion: muscles were conspicuously thin and unfused myoblasts were present in large numbers (Fig. 1E, asterisk). Moreover, some muscles seemed to be unable to find their proper attachment sites within the epidermis (Fig. 1E, arrow). Mesodermal overexpression of *rst* mediated by *twist-Gal4* (Baylies and Bate, 1996), *24B-Gal4* (Brand and Perrimon, 1993) or *twist-Gal4; 24B-Gal4* drivers neither caused lethality nor scorable muscle phenotypes. Ectodermal expression using *69B-Gal4* (Castelli-Gair et al., 1994) did not cause obvious phenotypes, except for some unfused myoblasts attached to the epidermis still present in stage 16 (data not shown).

Removal or truncation of Rst causes mild muscle defects: *rst* is not essential for muscle development

As overexpression of Rst causes dramatic muscle defects and lethality, we analysed *rst* mutants in detail. Loss of Rst protein in rst^{irreC1} (Schneider et al., 1995) was not lethal. However, embryos homozygous for rst^{irreC1} did show mild muscle defects. Individual muscles were missing in some, but not in all segments (Fig. 1F, arrowheads). Embryos homozygous for the allele rst^{6}, carrying a truncated version of the intracellular domain of Rst (Ramos et al., 1993), showed thin muscles and sometimes lacked them entirely (Fig. 1G, arrowhead) in some segments. Furthermore, rst^{6} embryos exhibited muscles in ectopic positions (Fig. 1G, arrow).

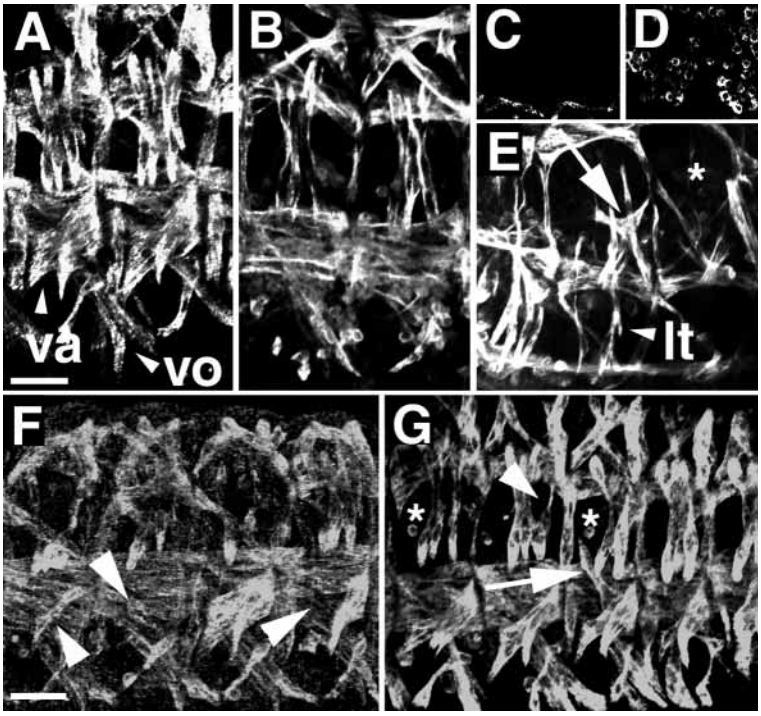

Fig. 1. Rst overexpression and mutant phenotypes in the stage 16 abdominal muscle pattern. Three dimensional reconstructions of confocal stacks of antibody staining against β-3-tubulin. Anterior is to the left and dorsal is upwards. (A) Heatshocked *yw* embryo. Arrowheads indicate ventral acute (va) and ventral oblique (vo) muscles. (B) Heatshocked *pCa18ZΔ3.1* embryo. Muscles are thin and some are missing (e.g. ventral acute muscles). (C) Heatshocked *yw* embryo. Single confocal plane interior to the muscles. (D) Heatshocked *pCa18ZΔ3.1 1* embryo. Single confocal plane as in C, showing a large amount of unfused fusion-competent myoblasts. (E) *da-Gal4/+;UAS-rst/+* embryo showing unfused fusion-competent myoblasts (asterisk), thin muscles and some muscles with ectopic projections (arrow). Several muscles are missing. lt, lateral transversal muscle. (F) rst^{irreC1} mutant embryo showing missing and thin muscles (arrowheads). (G) rst^{6} mutant embryo with misled (arrow) and thin muscles (arrowhead). Asterisks mark unfused fusion-competent myoblasts. Scale bars: 20 μm.

kirre, a locus highly related to *rst*

The *kirre* locus maps cytogenetically to region 3C6 and lies 3 kb distal to *Notch* (Fig. 2A). The *rst* and *kirre* loci are separated by 127 kb and are transcribed from opposite strands with their 5′ flanking regions towards each other (see Fig. 5A). The *kirre* cDNA consists of 3295 residues and contains a single long open reading frame encoding a protein of 959 amino acids. Algorithms by Sonnhammer et al. (Sonnhammer et al., 1998) and Nielsen et al. (Nielsen et al., 1997) identify a signal peptide sequence (amino acids 7-31) and one putative transmembrane region (amino acids 575-597).

The conceptual Kirre sequence shows an overall similarity of 45% to Rst (BLAST algorithm; Altschul et al., 1997). Like Rst, the predicted extracellular portion of the Kirre protein displays an array of five immunoglobulin (Ig) domains (Fig. 2B; Walsh and Doherty, 1997). Stretches of high conservation with Rst reside primarily in the region of the five Ig domains. Within these domains, the degree of conservation successively decreases from the N terminus to the transmembrane domain (Figs 2B,C; boundaries of Ig domains as in Ramos et al. (Ramos et al., 1993)). Both proteins contain stretches of amino acids with short side chains at differing positions (Fig. 2B, arrows): Rst contains a stretch of glycines between the second and third immunoglobulin-domain and Kirre harbours an array of 18 serines interrupted by a single glycine residue at the N terminus.

The intracellular domain of Kirre is considerably longer than that of Rst and displays only low overall homology with the one of Rst. However, three highly conserved motifs were detected (Fig. 2C): One is located close to the transmembrane domain consisting of the sequence PADVI. The second motif, R[Y/F]SAIYGNPYLR(S)[S/T]NSSLLPP, corresponds to the consensus sequence of autophosphorylation domains of receptor tyrosine kinases (Yarden and Ullrich, 1988). The third motif, T[A/H]V, resides at the C terminus of both sequences and corresponds to the consensus sequence of the PDZ-binding motif ([T/S]XV; Garner et al., 2000). In addition to the site contained in the putative autophosphorylation domain, one putative tyrosine and one putative serine phosphorylation site are conserved between Rst and Kirre (NetPhos 2.0 algorithm) (Blom et al., 1999). A conspicuous difference between the Kirre and Rst proteins is the lack of the *opa*-like repeat of Rst in Kirre (Ramos et al., 1993).

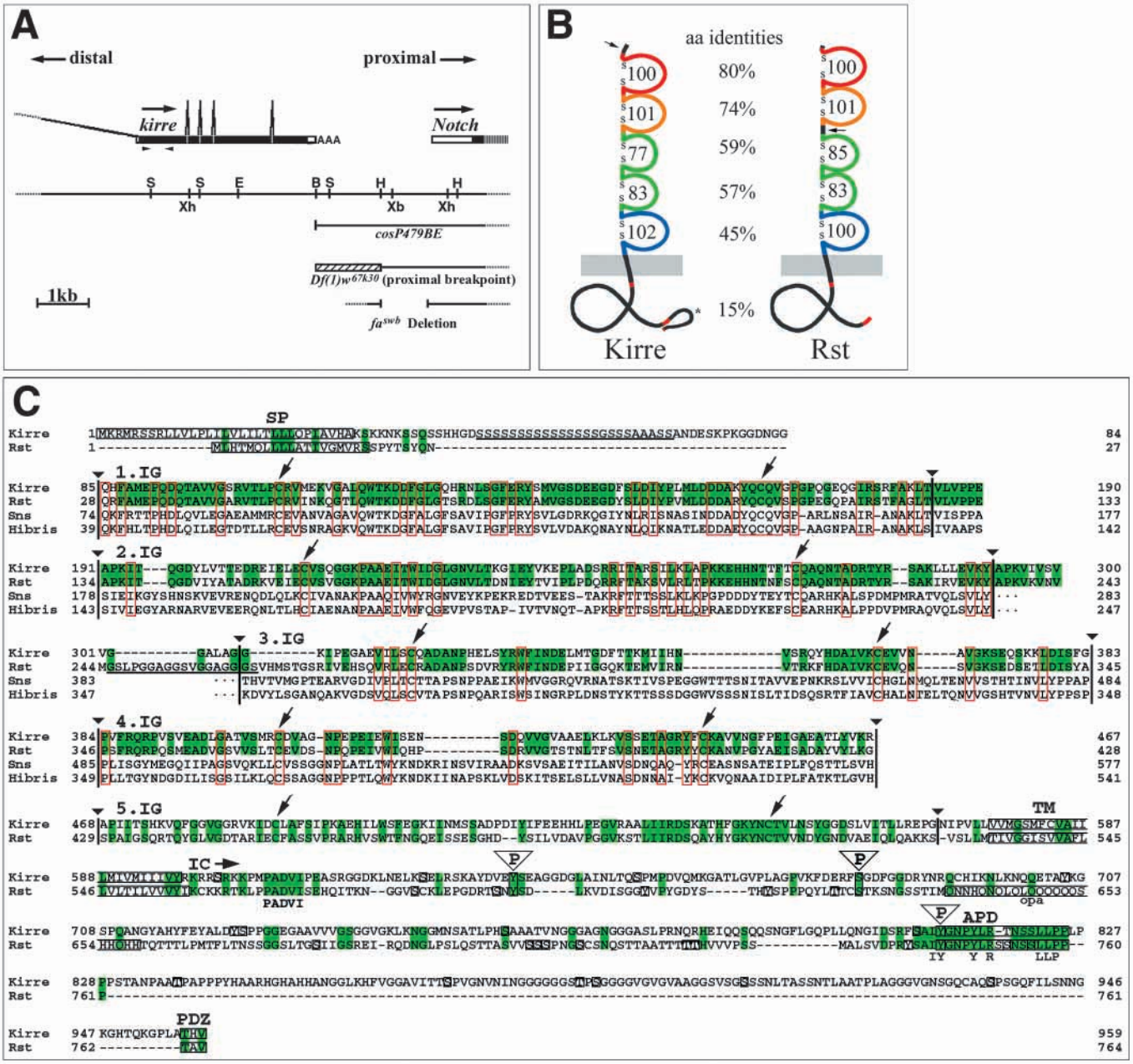

Fig. 2. The *kirre* and *rst* genes and proteins. (A) Physical map of the *kirre* locus. The first exon of *kirre* resides about 30 kb distal and is not depicted. Unbroken lines symbolize genomic DNA present in the depicted deficiency chromosomes and the *cosP479BE* transgene. Hatched bars refer to the closest possible breakpoint predictions. Arrowheads symbolize *kirre*-specific primers used in single fly PCR. Open reading frames are depicted as black bars and orientation of transcription by arrows. Restriction sites: B, *Bgl*II; E, *Eco*RI; H, *Hin*dIII; S, *Sac*I; Xb, *Xba*I; Xh, *Xho*I. (B) Schematic comparison of the Rst and Kirre proteins. Numbers refer to sizes of Immunoglobulin (Ig) domains and to percentages of sequence identities of paralogous Ig domains, respectively. Arrows indicate the serine- and glycine-rich repeats of Kirre and Rst, respectively. An asterisk marks the sequence stretch separating the autophosphorylation domain and the PDZ-binding motif in Kirre. (C) Alignment of Rst, Kirre, Sns and Hibris. Residues identical in Rst and Kirre are on green background, residues identical within all four sequences are boxed in red. Borders of Ig domains (Ramos et al., 1993) are marked by a vertical bar and an inverted triangle. Arrows indicate cysteines involved in forming a disulphide bond. Serine- and glycine-rich repeats of Kirre and Rst, respectively, are underlined. Putative phosphorylation sites conserved within Kirre and Rst are marked by P in an inverted triangle. Unconserved sites are boxed. APD, autophosphorylation domain with consensus sequence below; IC, intracellular domain; IG, Immunoglobulin domain; PADVI, conserved motif; opa, *opa*-like repeat; PDZ, PDZ-binding motif; SP, signal peptide; TM, transmembrane domain. Boxed sequence stretches contain the corresponding patterns.

Similarity searches using the BLAST algorithm showed that the four N-terminal Ig domains of Kirre, Rst, Sns (Bour et al., 2000) and Hibris (GenBank Accession Number, AF210316) are closely related (Fig. 2C). Sns and Hibris have been shown to be involved in muscle development (Bour et al., 2000) (H. A. Dworak and H. Sink, personal communication).

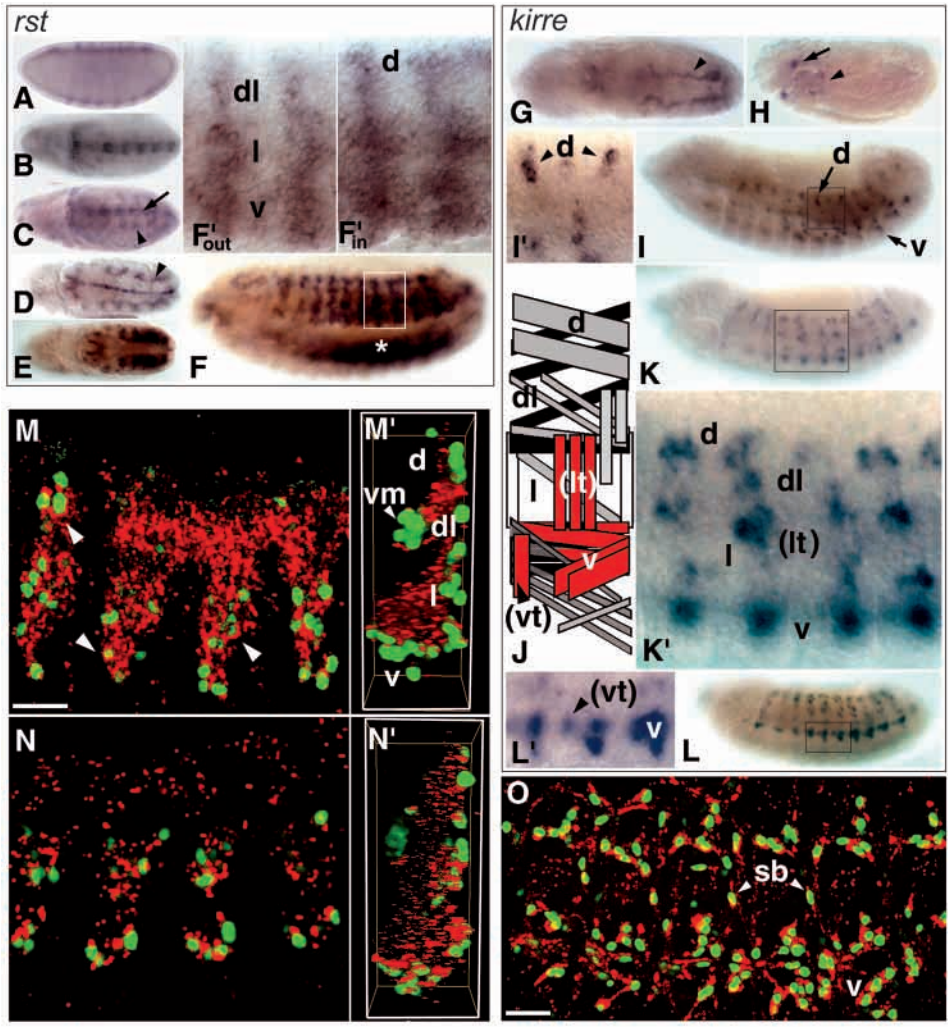

Fig. 3. Comparative analysis of *rst* and *kirre* expression patterns. Anterior is towards the left. Dorsal is upwards for A,I,K (lateral view) and F,H,L (ventrolateral view). (B-E,G) Dorsal view. (A-F) *rst* in situ hybridization. (A) Expression of *rst* starts during stage 4 in seven stripes enveloping the embryo. Soon thereafter this pattern fades and *rst* is expressed dorsally in procephalic regions and in the future amnioserosa, while ventrally the striped pattern remains present during invagination of the ventral furrow (data not shown). (B) At stage 8, *rst* labels a segmental pattern in mesectodermal cells. (C) During stage 9, *rst* is expressed in the midline (arrow) and mesodermal cell clusters (arrowhead). (D) At stages 10 to 11, the staining in the midline increases and *rst* starts to label progenitors of the visceral muscles (arrowhead). (E) At stage 12, the midline staining fades and *rst* is expressed strongly in the majority of mesodermal cells. (F) At stages 13-14, *rst* labels segmental stripes of mesodermal cells close to the epidermis. (F′$_{out}$) Focal plane close to the epidermis: *rst* expression includes regions where founder cells reside. dl, dorsolateral; l, lateral; v, ventral clusters (d, dorsal cluster out of focus in F'$_{out}$). (F'$_{in}$) Focal plane somewhat further interior within the mesoderm: *rst* is expressed where fusion-competent myoblasts reside. (G-L) *kirre* in situ hybridization. (G) Expression of *kirre* starts during stage 11 in the progenitors of the visceral muscles (arrowhead). (H) *kirre* expression can be detected up to stage 16, when *kirre* labels a ventral u-shaped structure at the posterior end of the head region (arrowhead) and two regions more anterior (arrow). (I) During stages 12 to 13, *kirre* is expressed in segmental clusters close to the epidermis at positions where founder cells reside. (I') Higher magnification of the boxed region in I, showing *kirre* expression in the dorsal group of muscle founder cells (d). (J) Scheme of the larval muscle pattern. Depicted in red are muscle groups that can be identified in K′,L′. (K,K′,L,L′) Expression of *kirre* in outgrowing muscle founder cells/precursors in stage 13-14. lt, lateral transversal muscle precursor; vt, ventral transversal precursor. (M-O) Rst antibody staining of abdominal hemisegments of embryos of the *rP298lacZ* enhancer trap line. Green labels β-galactosidase-expressing nuclei and red highlights Rst signal. (M) Single confocal plane within somatic mesoderm of a stage 13-14 *rP298lacZ* embryo. Arrowheads indicate cells labelled for Rst and β-galactosidase. (M′) Reconstruction of one hemisegment viewed from anterior. Position and morphology of Rst-labelled cells that do not express β-galactosidase strongly suggests that these cells are fusion-competent myoblasts. vm, visceral muscles. (N,N′) Staining of stage 13 to 14 *rP298lacZ* embryos in a *mbc*^{C1} background are roughly comparable with M,M′. (O) In older embryos of the same genotype, Rst expression can be detected in fibrous cells expressing β-galactosidase (founder cells), while it is very weak in fusion-competent myoblasts. v, ventral founder cells; sb, founder cell of segment border muscle. Scale bars: 20 μm.

The spatial expression patterns of *rst* and *kirre* overlap in muscle founder cells

We performed in situ hybridization using probes specific for *kirre* and *rst*, respectively (see Materials and Methods), to identify temporal and spatial expression domains for both genes.

Expression of *rst* mRNA could be detected in embryonic stages 4 to 14 (Fig. 3A-F) (Ramos et al., 1993). During stage 12, the *rst* transcript was detected in the majority of mesodermal cells (Fig. 3E). During stages 13 to 14 mesodermal expression of *rst* could be detected close to the epidermis at positions where muscle founder cells reside (Fig. 3F′$_{out}$), as well as immediately interior of the founder cells where fusion-competent myoblasts can be found (Fig. 3F, asterisk, Fig. 3F′$_{in}$). Unlike for *kirre*, we were never able to identify individual muscle precursors based on *rst* labelling.

In comparison with *rst*, the expression of *kirre* is more restricted and switched on later during development. The *kirre* mRNA was detected from stage 11 through to stage 16 (Fig. 3G-L). During stages 12-13, the *kirre* probe labelled segmental clusters of mesodermal cells close to the epidermis. Based on position and morphology, this suggests that *kirre* is expressed in muscle founder cells (Fig. 3I,I′). During stages 13 to 14, *kirre* labelled outgrowing founder cells and muscle precursors (Fig.

3K,K′,L,L′). Our data regarding *kirre* localization reconfirm results reported by Ruiz-Gomez et al. (Ruiz-Gomez et al., 2000).

A monoclonal antibody against Rst (Schneider et al., 1995) was used to address protein expression in more detail. Crossreactivity of this antibody with Kirre was ruled out by the complete absence of staining of embryos homozygous for the *rst* null allele rst^{irreC2} (see Fig. 5A). As the proximal breakpoint of this inversion lies within the second intron of the *rst* gene, it should leave expression of *kirre* unimpaired, which resides about 127 kb more proximal. Moreover, staining of wild-type embryos using this antibody reconfirmed *rst* in situ hybridization patterns.

To determine the myogenic cell types expressing Rst, we used the muscle founder cell-specific enhancer trap line *rP298-lacZ* (Nose et al., 1998). During embryonic stages 13 to 14, all cells expressing β-galactosidase also showed Rst staining in their periphery (Fig. 3M), indicating that Rst is expressed by muscle founder cells. As predicted by in situ hybridization, Rst was also detected in mesodermal cells that did not express β-galactosidase. Morphology and position of these cells suggest that they are fusion-competent myoblasts (Fig. 3M′). The localization of Rst within the membranes of myogenic cells was restricted to discrete spots (Fig. 3M,N).

In *rP298-lacZ* embryos, fusion-competent myoblasts that have started to fuse with founder cells begin to express β-galactosidase. This complicates the distinction between the two cell types. To determine whether Rst is expressed in isolated founder cells, we crossed *rP298-lacZ* into a mbc^{C1} genetic background (Fig. 3N-O). In mbc^{C1} embryos, myoblast fusion is almost completely blocked and by stage 16 these embryos display a pattern of isolated, globular, fusion-competent myoblasts and stretched out, fibrous muscle founder cells (Rushton et al., 1995). By stages 13 to 14, antibody staining for β-galactosidase and Rst revealed a pattern comparable with staining in a wild-type background (Fig. 3N,N′). However, during stages 15 to 16, Rst expression on fusion-competent myoblasts almost completely disappeared, while labelling was pronounced on the cytoplasmic extensions of founder cells (Fig. 3O). Moreover, as *rP298lacZ* mirrors *kirre* expression (Ruiz-Gomez et al., 2000), it follows that the expression patterns of *rst* and *kirre* overlap.

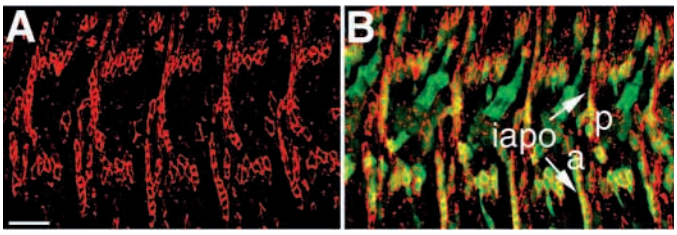

Fig. 4. Rst is expressed in the apodemes. Double staining of abdominal hemisegments of the *Wβ1HI-lacZ* apodeme specific enhancer trap line shows overlap during stage 14: (A) Rst channel. (B) Overlay of Rst (red) and β-galactosidase (green). a, anterior; iapo, intersegmental apodemes; p, posterior. Scale bar: 20 μm.

Muscles attach at specific sites in the epidermis, the apodemes. Rst is also expressed in the apodemes (Fig. 4), as shown by immunodetection of Rst in embryos of the apodeme-specific *lacZ*-reporter *Wβ1HI-lacZ* (Buttgereit, 1993).

Deletion of *kirre* does not cause obvious muscle defects: *kirre* is not essential for muscle development

We used combinations of available chromosomal rearrangements to generate flies deficient for the *kirre* gene. Several deletions are available that remove the *Notch* locus and varying stretches of the genomic area 5′ of *Notch* (Fig. 5A). In order to obtain *kirre*-deficient males, we combined $Df(1)N^{54l9}$ (Lefevre and Green, 1972; Perlman, 1983) with the transgene *cosP479BE* (Fig. 5A) that rescues the *Notch* function (Ramos et al., 1989). Similarly, *kirre*-deficient females were generated by placing $Df(1)N^{54l9}$ in *trans* over $Df(1)w^{67k30}$. The latter deficiency removes the genomic region, including subdivisions 3C2 to 3C6 that contain *w, rst* and *vt* (Fig. 5A) (Lefevre and Green, 1972). The proximal breakpoint is located just proximal to the region where *kirre* is located and leaves *Notch* intact (Fig. 2A) (Grimwade et al., 1985). The progeny of both crosses carry at least one wild-type copy of *Notch* and hence rescue the *Notch*-dependent lethality.

As reported previously (Lefevre and Green, 1972; Ramos et al., 1989), both crosses give rise to viable adult flies. We

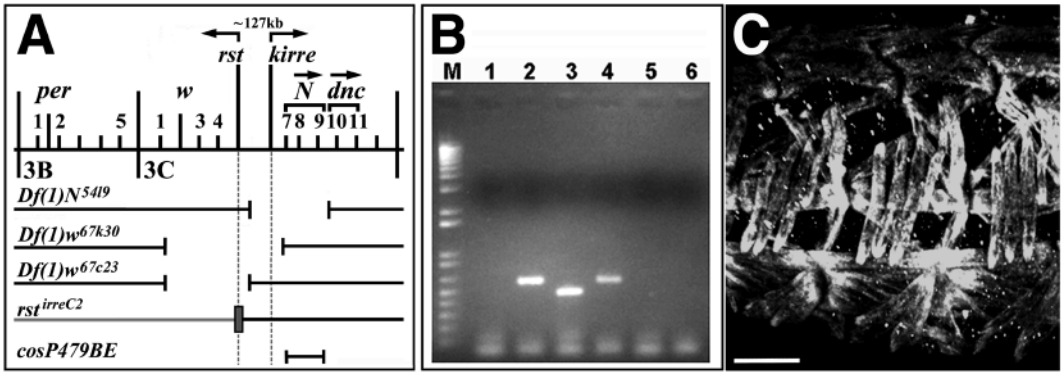

Fig. 5. *kirre* is not essential for muscle development. (A) Schematic depiction of the *white-Notch* region and deficiencies used in this study (see text). $Df(1)w^{67c23}$ is a viable deletion removing 3C2-5 (Lefevre and Green, 1972; see discussion). (B) Single fly PCR proves that *kirre* is not present in the genome of $Df(1)N^{54l9}/Y;cosP479BE/+$ flies. Lanes 1,3,5: *kirre*-specific primers. Lanes 2,4,6: *rst*-specific primers. Lanes 1,2: $Df(1)N^{54l9}/Y;cosP479BE/+$ as template. Lanes 3,4: wild-type Berlin males as template. Lanes 5,6: no template. (C) Abdominal muscle pattern of $Df(1)N^{54l9}/Y;cosP479BE/+$ embryo stained for muscle Myosin is indistinguishable from wild type. Anterior is towards the left, dorsal is upwards. Scale bar: 20 μm.

performed single fly PCR on *Df(1)N^{54l9}/Y;cosP479BE/+* males to confirm the absence of the *kirre* locus in *Df(1)N^{54l9}*. The experiments reproducibly failed to reveal an amplification product using *kirre*-specific primers (Fig. 2A, arrowheads; Fig. 5B, lane 1), while the same primers gave rise to PCR products on wild-type males (Fig. 5B, lane 3). PCR with *rst* specific primers used as controls for the integrity of the DNA preparation always showed amplification products on the same *Df(1)N^{54l9}/Y; cosP479BE/+* DNA preparations used with the *kirre*-specific primers (Fig. 5B, lane2) and also on wild-type control males (Fig. 5B, lane 4).

To reveal a putative muscle phenotype of *kirre*-deficient embryos, we analysed the muscles of non-balanced embryos. We were unable to find defects (Fig. 5C). The GFP balancer we used for selection of the appropriate genotypes (*FM7i,P{w^{+mC}=ActGFP}JMR3*) does not allow clear distinction between balanced and non-balanced embryos before stage 16-17 because of a strong maternal contribution of GFP. To rule out the possibility of *kirre*-deficient embryos displaying a muscle phenotype that arrests development before these stages, we analysed 110 embryos resulting from a cross *Df(1)N^{54l9}/FM6* x *X/Y;cosP479BE* by anti-Myosin staining and confocal microscopy. Aside from the expected *Notch* phenotypes, no defects were detectable with this antibody (data not shown). The deficiency *Df(1)N^{54l9}* does not extend into the *rst* locus, as *Df(1)N^{54l9}/rst^{6}* females do not display the *rst* eye phenotype of *rst^{6}* (data not shown).

A *kirre, rst* double mutant is lethal and shows severe muscle defects

The deficiency *Df(1)w^{67k30}* causes embryonic lethality and displays an almost complete lack of myoblast fusion (Fig. 6; Ruiz-Gomez et al., 2000). The genomic interval removed by *Df(1)w^{67k30}* extends from *white* to *kirre*. As yet, there is no single embryonic lethal locus known within this region. Hence, the *Df(1)w^{67k30}* phenotype could be caused by the removal of two or several loci. Kirre has been shown to be a myoblast attractant expressed on founder cells and reintroduction of *kirre* can partially rescue the *Df(1)w^{67k30}* phenotype (Ruiz-Gomez et al., 2000). Therefore, removal of *kirre* is partly responsible for the *Df(1)w^{67k30}* phenotype. However, as shown above, embryos deficient for a smaller genomic region including *kirre* do not show a defect in myoblast fusion. Therefore, removal of *kirre* alone cannot be responsible for the *Df(1)w^{67k30}* phenotype. As the situation for *rst* is similar – *rst* is involved in but not essential for myoblast fusion – we conclude that the phenotype of *Df(1)w^{67k30}* is caused by the simultaneous removal of the *rst* and *kirre* loci.

Reintroduction of *rst* rescues the *Df(1)w^{67k30}* phenotype

To test the hypothesis that the *Df(1)w^{67k30}* phenotype is partially caused by the removal of the *rst* locus, we reintroduced *rst* into the mesoderm of *Df(1)w^{67k30}* embryos (Fig. 7) using the UAS/Gal4-system. We used *twi-Gal4* as a driver, which mediates expression within the entire mesoderm from gastrulation up to late stage 11, when the expression becomes restricted to somatic muscles and to the heart (Baylies and Bate, 1996). Expression of *rst* under the control of the *twi-Gal4* driver in the background of *Df(1)w^{67k30}* almost completely restored the wild-type muscle pattern (Fig. 7B).

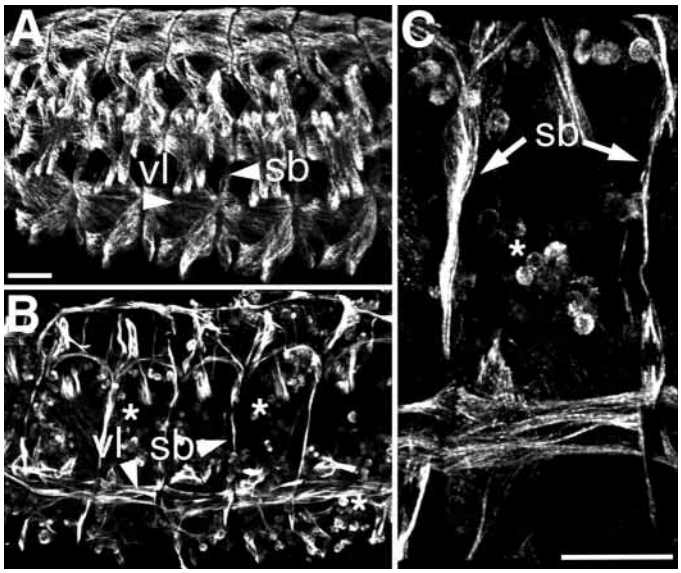

Fig. 6. *Df(1)w^{67k30}* is a *rst, kirre* double mutant and shows severe muscle defects. (A) Wild-type abdominal muscle pattern as revealed by staining against β-3-tubulin. vl, ventral longitudinal muscles; sb, segment border muscle. (B) *Df(1)w^{67k30}* embryos display a drastic myoblast fusion phenotype with thin outgrowing muscle founder cells and many unfused myoblasts (asterisks). (C) Detailed view of two abdominal hemisegments of the same embryo. Scale bars: 20 μm.

The muscle pattern of the rescued embryos displayed only small defects such as ectopically projecting or thinner muscles (Fig. 7B, arrow and asterisk). We conclude that *rst* alone is sufficient to rescue the *Df(1)w^{67k30}* phenotype. As the same has been shown for *kirre* (Ruiz-Gomez et al., 2000), this supports the hypothesis that the *Df(1)w^{67k30}* phenotype is caused by the simultaneous removal of *rst* and *kirre*.

Rst is a myoblast attractant

Ectopically expressed Kirre recruits fusion-competent myoblasts to ectopic sites in a background null for both *rst* and *kirre* (Ruiz-Gomez et al., 2000). If Rst and Kirre are functionally equivalent during myoblast fusion, Rst should also be sufficient for ectopic recruitment of fusion-competent myoblasts. We tested this hypothesis (Fig. 8) using the same driver lines as were used for Kirre, *wg-Gal4* (Glise and Noselli, 1997) and *dll-Gal4* (Calleja et al., 1996).

The cross *Df(1)w^{67k30}/w; dll-Gal4/+* x *w/Y; +/+; UAS-rst* yielded progeny hemi- and heterozygous for *Df(1)w^{67k30}*. In a *Df(1)w^{67k30}* background, overexpression of Rst driven by *dll-Gal4* recruited myoblasts to the epidermis analogous to the results for Kirre. Fusion-competent myoblasts that would normally reside further inside the embryo are attracted towards the sites of ectopic Rst expression in the leg discs and in the head region (Fig. 8B,C). Embryos that carry at least one non-deficiency X-chromosome, albeit not defective in myoblast fusion, also displayed attraction of fusion-competent myoblasts to sites of ectopic Rst expression (Fig. 8D-I). These myoblasts were still present in late stages (around stage 16), when embryos from the same cross that did not express Rst ectopically displayed none or only few unfused myoblasts. Misexpression of Rst under the control of the *wg-Gal4* line in a wild-type genetic background yielded comparable results:

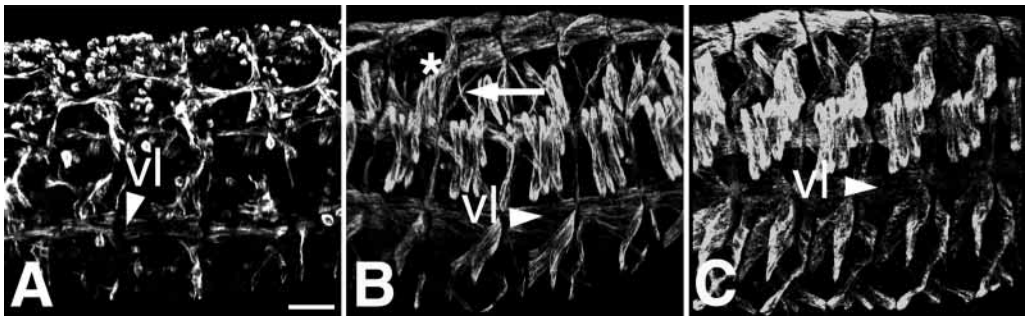

Fig. 7. Reintroduction of Rst into the mesoderm rescues the phenotype of *Df(1)w*^{67k30}, *N*$^{fa\text{-}g}$ embryos (see Materials and Methods). (A) *Df(1)w*^{67k30}, *N*$^{fa\text{-}g/Y}$ embryo displaying a strong myoblast fusion phenotype. (B) *Df(1)w*^{67k30}, *N*$^{fa\text{-}g/Y}$, *twi-Gal4* x *UAS-rst* embryo displaying a nearly wild-type abdominal muscle pattern with minor defects: some muscles are thin (arrow) and some terminate in ectopic positions (asterisk). (C) Hetero- or homozygously balanced embryo out of the same cross (indistinguishable from wild-type). vl, ventral longitudinal muscles. Scale bar: 20 μm.

fusion-competent myoblasts were attracted to the epidermis in areas where Rst was ectopically expressed. During stage 16 these myoblasts were still present and resided exterior to the developing ventral acute muscles (Fig. 8K,L).

As Rst is expressed in the apodemes, it remains unclear why fusion-competent myoblasts do not attach to apodeme cells. However, Rst could be detected at sites of ectopic expression in much higher quantities than in the apodemes (Fig. 8M) and closer analysis of different confocal sections revealed that Rst in apodeme cells resides primarily in rings around the apical domains (Fig. 8M,N) of apodeme cells, and not basally, where fusion-competent myoblasts would be suspected to make contact.

DISCUSSION

The Kirre and Rst proteins are closely related

Rst and Kirre are highly related proteins. In the extracellular domain, all Ig domains display relatively high conservation, with the first two domains being most similar. In contrast to Ruiz-Gomez et al. (Ruiz-Gomez et al., 2000), we also detected three motifs of very high sequence conservation in the intracellular domain. Interestingly, two of these motifs may be functionally relevant in signalling processes: one contains the consensus sequence for autophosphorylation domains of ligand-dependent tyrosine kinases (Yarden and Ullrich, 1988). As we have no indication that Rst or Kirre display kinase

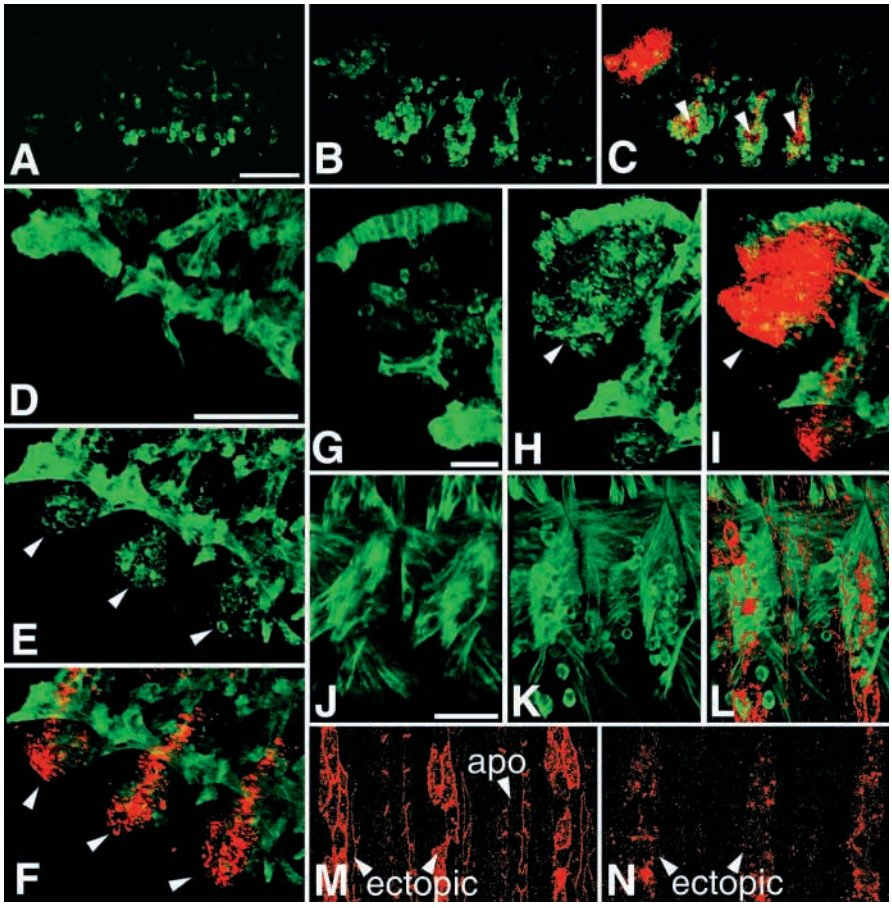

Fig. 8. Ectopic expression of Rst attracts myoblasts to ectopic sites. Embryos are stained in green for muscle-specific markers ((A-C,J-L) β-3-tubulin (D-I) muscle myosin) and for Rst in red. (C,F,I,L) Merged images. (A) *Df(1)w*^{67k30}, *N*$^{fa\text{-}g}$ embryo: only very few myoblasts can be found close to the epidermis. (B,C) *Df(1)w*^{67k30}, *N*$^{fa\text{-}g}$; *dll-Gal4/+*, *UAS-rst/+* embryo: attraction of myoblasts towards the epidermis around legdiscs (arrowheads). (D-I) Embryos from the same cross, which are either heterozygous or homozygous for the balancer. (D,G) Embryo not misexpressing Rst. (E,F,H,I) *dll-Gal4/+*, *UAS-rst/+* embryos: ectopic myoblasts cluster in ventral regions of the thoracal segments up to stage 16 (E,F, arrowheads) and in the head region (H,I, arrowheads). (J) *wg-Gal4/wg-Gal4* control embryo. (K,L) *wg-Gal4/UAS-rst* embryo: attraction of myoblasts to epidermal sites distal to the ventral acute muscles. (M,N) Two single focal planes through the epidermis: (M) apical position; (N) 2,5 μm below. Rst labels basal membranes of epidermal cells only at sites of ectopic expression (ectopic) and only very weakly in apodemes (apo). Scale bars: 20 μm.

activity, we propose a putative as yet unknown interaction partner to do so. Additionally, a C-terminal stretch corresponds to the PDZ-binding motif, which may have implications for the subcellular localization of the proteins (Garner et al., 2000). Indeed, Rst distribution in all tissues studied so far shows strong subcellular localisation.

The expression patterns of *rst* and *kirre* overlap, but are not identical

Expression patterns of *rst* and *kirre* overlap in muscle founder cells. With regard to *kirre*, our results confirm those of Ruiz-Gomez et al. (Ruiz-Gomez et al., 2000), showing expression in founder cells and muscle precursors. As for *rst*, the expression is more widespread and includes, in addition to expression in founder cells, fusion-competent myoblasts.

Although Rst immunoreactivity is present in founder cells, we could not unequivocally identify individual outgrowing precursors based on Rst staining, because of subcellular localization and the strong expression of Rst in fusion-competent myoblasts directly adjacent. However, on identification of precursors by staining for β-3-tubulin, a weak residual Rst immunoreactivity can initially be detected in precursors until the end of stage 13, which fades soon thereafter (data not shown). With regard to the muscle precursors, this downregulation of Rst seems to be dependent on the occurrence of muscle fusion. In contrast to wild type, Rst is still expressed on founder cells at stage 16 in a mbc^{C1} background (Fig. 3O), where myoblast adhesion is almost completely blocked (Rushton et al., 1995). In fusion-competent myoblasts, however, Rst is downregulated in a mbc^{C1} background, with large numbers of unfused fusion-competent myoblasts still being present at that stage. This asymmetry in regulation of Rst expression in both cell types is noteworthy. Fusion-dependent downregulation of Rst in muscle precursors could function in size regulation of muscles.

Rst overexpression and mutant phenotypes

Although the *rst* gene is not essential for muscle fusion, small defects like thinner and missing muscles can be detected in rst^{6} and rst^{irreC1} individuals, indicating the involvement of *rst* in muscle development.

Overexpression of a secretable, extracellular version of Rst during stages when myoblast fusion occurs (stages 12-15) leads to embryonic lethality and defects in myoblast fusion. Mechanistically, the extracellular part of the protein may compete with endogenous Rst for an as yet unknown extracellular ligand or, as the Rst protein has been shown to mediate homophilic cell adhesion (Schneider et al., 1995), the extracellular domain could also bind to endogenous Rst and thereby disturb its function.

Ubiquitous overexpression of the full-length Rst protein also caused embryonic lethality and a severe muscle fusion phenotype. Ectodermal overexpression of Rst did not cause defects in the muscle pattern but ectopic localization and prolonged occurrence of myoblasts at sites of ectopic Rst expression. Mesodermal expression did not induce any detectable phenotype. The reason why global misexpression of Rst differs from misexpression in the mesoderm alone (in most of which Rst is expressed anyway) and from misexpression in the ectoderm alone appears to be the increase of Rst expressing sticky surfaces: the withdrawal of fusion-competent myoblasts from recruiting founders and precursors may considerably lower the probability for these cell types to contact each other.

Some of the defects observed in *rst* mutants concern muscles in ectopic positions (Fig. 1E,G, arrows). Even though Rst is expressed in the apodemes, our data do not point to an essential role for *kirre* and/or *rst* in myotube guidance or attachment: analysis of the subcellular localization shows accumulation of Rst primarily around the apical borders of the apodemes, rather than basally, where outgrowing muscles would be expected to make contact. Moreover, apodeme specification is also not blocked in individuals lacking ectodermal Rst and Kirre, as judged by the muscle pattern (Fig. 7B). Hence, a putative function of Rst in apodeme specification would be redundantly safeguarded by additional as yet unknown factors. Apodeme specification is also not disrupted in *da-Gal4/+;UAS-rst/+* embryos, as revealed by antibody staining against Alien (Goubeaud et al., 1996; data not shown). This clearly rules out the possibility that the strong muscle phenotype observed in these embryos is due to defects in specification of the muscle attachment sites, and argues that restricted expression of Rst is not essential for normal apodeme specification to occur. This is underlined by the fact that *69B-Gal4/+;UAS-rst/+* embryos that express Rst only in the ectoderm do not show attachment defects (data not shown).

Simultaneous deletion of *kirre* and *rst* blocks myoblast fusion

The deficiency $Df(1)w^{67k30}$ deletes the genomic region 3C2-3C6, including *rst* and *kirre*. It has been reported previously that $Df(1)w^{67k30}$ is associated with a lethal myoblast fusion phenotype (Ruiz-Gomez et al., 2000). Our analysis of flies deficient for *kirre*, but not for *rst*, revealed that neither *kirre* nor *rst* alone are essential for myoblast fusion. Moreover, reintroduction of *rst* into the mesoderm restored the $Df(1)w^{67k30}$ phenotype to almost wild-type, as has been shown for *kirre* (Ruiz-Gomez et al., 2000). Hence, one copy of either *rst* or *kirre* is sufficient to restore the wild-type muscle pattern. Furthermore, ectopic expression of Rst mediated ectopic recruitment of fusion-competent myoblasts as has been shown with Kirre (Ruiz-Gomez et al., 2000). Given the overlapping mesodermal expression patterns of *rst* and *kirre*, and the significant structural similarity between the two proteins, we conclude that *rst* and *kirre* have at least partially redundant functions during muscle development.

Our findings may provide a molecular basis for the findings of Lefevre and Green (Lefevre and Green, 1972), who proposed a genetic duplication between 3C2-5 (the *rst* locus resides at 3C5) and 3C6: individuals are viable when either one of the regions 3C2-5 or 3C6 is deleted; however, they die when both are missing (Fig. 5A). Even though *kirre* is now mapped to 3C7 (FlyBase – http://flybase.bio.indiana.edu), the mapping data of Lefevre and Green can account for *kirre*, since other mapping data put the *kirre* locus into 3C6: the 5′ end of *Notch* was mapped in between 3C6 and 3C7 (Rykowski et al., 1988) and the fa^{swb} deletion, which resides in between *kirre* and *Notch* (Fig. 2A) (Ramos et al., 1989), has been shown to fuse 3C6 and 3C7 (Keppy and Welshons, 1976).

Rst, Kirre and the fusion machinery

Rst expression in fusion-competent myoblasts is not essential for their attraction towards ectopic Kirre or Rst: myoblasts can

be attracted to ectopic sites in a *Df(1)w*^{67k30} background, where Rst is only present at ectopic sites and not in fusion-competent myoblasts – thus strongly suggesting a heterophilic *trans*-interaction. However, as Rst has been shown to mediate homophilic cell adhesion (Schneider et al., 1995), a homophilic *trans*-interaction of Rst may also contribute to the fusion process.

At present, the data do not allow a prediction of the molecular mechanisms in which Rst and Kirre take part; however, it is conceivable that they include the related cell adhesion molecules Sns and Hbs that are expressed on fusion-competent myoblasts (Bour et al., 2000) (H. A. Dworak and H. Sink, personal communication). A model of the fusion machinery may include assembly of adhesion molecules within heteromeric complexes with differing compositions on the side of the fusion-competent myoblasts (including Sns, Hbs and Rst) and on the founder cells (including Kirre and Rst). These complexes may still function after loss of single components. It will need further analysis and binding assays to elucidate how these membrane proteins play together and how they are connected to the other components of the fusion machinery.

We acknowledge the technical assistance by M. S. A. Costa, M. Böhler, W. Brinkmann and M. S. Z. Graeff. Thanks to D. P. Kiehart, R. Renkawitz-Pohl, S. Artavanis-Tsakonas, M. Bate, M. Calleja and S. Noselli for antibodies and/or fly strains, and G. Igloi for sequencing. M. S. and B. B. are indebted to all members of the Department of Morphology, USP-Ribeirao Preto, Brazil for great hospitality and to M. Hoehne for careful reading of the manuscript and discussion. This work was supported by the SFB 388 (to K. F. F.), FAPESP (Grants #96/06235-2 and #00/07874-3 to R. G. P. R.) and DAAD/CAPES (PROBRAL 2000) to M. S., B. B. and K. F. F.

REFERENCES

Altschul, S. F., Madden, T. L., Schäffer, A. A., Zhang, J., Zhang, Z., Miller, W. and Lipman, D. J. (1997). Gapped BLAST and PSI-BLAST: a new generation of protein database search programs. *Nucleic Acids Res*. **25**, 3389-3402.

Ashburner, M. (1989). Drosophila – *A Laboratory Manual*. Cold Spring Harbor, New York: Cold Spring Harbor Laboratory Press.

Bate, M. (1990). The embryonic development of larval muscles in *Drosophila*. *Development* **110**, 791-804.

Bate, M. (1993). The mesoderm and its derivatives. In *The development of* Drosophila melanogaster. Vol. 2 (ed. M. Bate and A. Martinez-Arias), p. 1013. Cold Spring Harbor, New York: Cold Spring Harbor Laboratory Press.

Baylies, M. K. and Bate, M. (1996). *twist*: a myogenic switch in *Drosophila*. *Science* **272**, 1481-1484.

Baylies, M. K., Bate, M. and Ruiz-Gómez, M. (1998). Myogenesis: a view from *Drosophila*. *Cell* **93**, 921-927.

Benos, P. V., Gatt, M. K., Ashburner, M., Murphy, L., Harris, D., Barrell, B., Ferraz, C., Vidal, S., Brun, C., Demailles, J. et al. (2000). From sequence to chromosome: the tip of the X chromosome of *D. melanogaster*. *Science.* **287**, 2220-2222.

Blom, N., Gammeltoft, S. and Brunak, S. (1999). Sequence- and structure-based prediction of eukaryotic protein phosphorylation sites. *J. Mol. Biol.* **294**, 1351-1362.

Bour, B., Chakravarti, M., West, J. M. and Abmayr, S. M. (2000). *Drosophila* SNS, a member of the immunoglobulin superfamily that is essential for myoblast fusion *Genes Dev.* **14**, 1498-1511.

Brand, A. H. and Perrimon, N. (1993). Targeted gene expression as a means of altering cell fates and generating dominant phenotypes. *Development* **118**, 401-441.

Buttgereit, D. (1993). Redundant enhancer elements guide *beta 1 tubulin* gene expression in apodemes during *Drosophila* embryogenesis. *J. Cell Sci.* **105**, 721-727.

Calleja, M., Morena, E., Pelaz, S. and Morata, G. (1996). Visualization of gene expression in living adult *Drosophila*. *Science* **274**, 252-255.

Campos-Ortega, J. A. and Hartenstein, V. (1997). *The Embryonic Development of* Drosophila melanogaster. 2nd edn. Berlin-Heidelberg: Springer Verlag.

Carmena, A., Bate, M. and Jiménez, F. (1995). *lethal of scute*, a proneural gene, participates in the specification of muscle progenitors during *Drosophila* embryogenesis. *Genes Dev.* **9**, 2373-2383.

Castelli-Gair, J., Greig, S., Micklem, G. and Akam, M. (1994). Dissecting the temporal requirements for homeotic gene function. *Development* **120**, 1983-1995.

Dieffenbach, C. W. and Dveksler, G. S. (1995). *PCR primer: A Laboratory Manual*. Cold Spring Harbor, New York: Cold Spring Harbor Laboratory Press.

Frasch, M. (1999). Controls in patterning and diversification of somatic muscles during *Drosophila* embryogenesis. *Curr. Opin. Genet. Dev.* **9**, 522-529.

Garner, C. C., Nash, J. and Huganir, R. L. (2000). PDZ domains in synapse assembly and signalling. *Trends Cell Biol.* **10**, 274-80.

Glise, B. and Noselli, S. (1997). Coupling of Jun amino-terminal kinase and decapentaplegic signaling pathways in *Drosophila* morphogenesis. *Genes Dev.* **11**, 1738-1747.

Goubeaud, A., Knirr, S., Renkawitz-Pohl, R. and Paululat, A. (1996). The *Drosophila* gene *alien* is expressed in the muscle attachment sites during embryogenesis and encodes a protein highly conserved between plants, *Drosophila* and vertebrates. *Mech. Dev.* **57**, 59-68.

Grimwade, B., Muskavitch, M. A. T., Welshons, W. J., Yedvobnick, B. and Artavanis-Tsakonas, S. (1985). The molecular genetics of the *Notch* locus in *Drosophila melanogaster*. *Dev. Biol*. **107**, 503-519.

Keppy, D. O. and Welshons, W. J. (1976). The cytogenetics of a recessive visible mutant associated with a deficiency adjacent to the Notch locus in *Drosophila melanogaster*. *Genetics* **85**, 497-506.

Kiehart, D. P. and Feghali, R. (1986). Cytoplasmic myosin from *Drosophila melanogaster*. *J. Cell Biol.* **103**, 1517-1525.

Lefevre, G. Jr. and Green, M. M. (1972). Genetic duplication in the *white-split* interval of the X chromosome in *Drosophila melanogaster*. *Chromosoma* **36**, 391-412.

Moda, L., Machado, R. and Ramos, R. G. P. (2000). Ubiquitous overexpression of a transgene encoding the extracellular portion of the *Drosophila* Roughest-Irregular Chiasm C protein induces early embryonic lethality. *An. Acad. Bras. Cienc.* **72**, 381-388.

Nielsen, H., Engelbrecht, J., Brunak, S. and von Heijne, G. (1997). Identification of prokaryotic and eukaryotic signal peptides and prediction of their cleavage sites. *Protein Eng.* **10**, 1-6.

Nose, A., Isshiki, T. and Takeichi, M. (1998). Regional specification of muscle progenitors in *Drosophila*: the role of the *msh* homeobox gene. *Development* **125**, 215-223.

Oxtoby, E. and Jowett, T. (1993). Cloning of the zebrafish *krox-20* gene *(krx-20)* and its expression during hindbrain development. *Nucleic Acids Res.* **21**, 1087-1095

Paululat, A., Holz, A. and Renkawitz-Pohl, R. (1999). Essential genes for myoblast fusion in *Drosophila* embryogenesis. *Mech. Dev*. **83**, 17-26.

Perlman, J. (1983). One side of a deletion breakpoint from the *Drosophila melanogaster* genome contains a transposable element. *Gene* **21**, 87-94.

Ramos, R. G. P., Grimwade, B. G., Wharton, K. A., Scottgale, T. N. and Artavanis-Tsakonas, S. (1989). Physical and functional definition of the *Drosophila Notch* locus by P element transformation. *Genetics* **123**, 337-348.

Ramos, R. G. P., Igloi, G. L., Lichte, B., Baumann, U., Maier, D., Schneider, T., Brandstätter, J. H., Fröhlich, A. and Fischbach, K.-F. (1993). *The irregular chiasm C-roughest* locus of *Drosophila*, which affects axonal projections and programmed cell death, encodes a novel immunoglobulin-like protein. *Genes Dev*. **7**, 2533-2547.

Reiter, C., Schimansky, T., Nie, Z. and Fischbach, K. F. (1996). Reorganization of membrane contacts prior to apoptosis in the *Drosophila* retina: the role of the IrreC-rst protein. *Development* **122**, 1931-1940.

Ruiz-Gómez, M., Coutts, N., Price, A., Taylor, M. V. and Bate, M. (2000). *Drosophila* dumbfounded: a myoblast attractant essential for fusion. *Cell* **102**, 189-198.

Rushton, E., Drysdale, F., Abmayr, S. M., Michelson, A. M. and Bate, M. (1995). Mutations in a novel gene, *myoblast city*, provide evidence in support of the founder cell hypothesis for *Drosophila* muscle development. *Development* **121**, 1979-1988.

Rykowski, M. C., Parmelee, S. J., Agard, D. A. and Sedat, J. W. (1988).

Precise determination of the molecular limits of a polytene chromosome band: Regulatory sequences for the *Notch* gene are in the interband. *Cell* **54**, 461-472.

Schneider, T., Reiter, C., Eule, E., Bader, B., Lichte, B., Nie, Z., Schimansky, T., Ramos, R. G. P. and Fischbach, K. F. (1995). Restricted expression of the Rst protein is required for normal axonal projections of columnar visual neurons. *Neuron* **15**, 259-271.

Sonnhammer, E. L. L., van Heijne, G. and Krogh, A. (1998). A hidden Markov model for predicting transmembrane helices in protein sequences. In *Proceedings of the Sixth International Conference on Intelligent Systems for Molecular Biology* (ed. J. Glasgow, T. Littlejohn, F. Major, R. Lathrop, D. Sankoff and C. Sensen), pp. 175-182. Menlo Park, CA: AAAI Press.

Tautz, D. and Pfeifle, C. (1989). A non-radioactive *in situ* hybridization method for the localization of specific RNAs in *Drosophila* embryos reveals translational control of the segmentation gene *hunchback*. *Chromosoma* **98**, 81-85.

Walsh, F. S. and Doherty, P. (1997). Neural cell adhesion molecules of the immunoglobulin superfamily: role in axon growth and guidance. *Annu. Rev. Cell Dev. Biol*. **13**, 425-456.

Wodarz, A., Hinz, U., Engelbert, M. and Knust, E. (1995). Expression of *crumbs* confers apical character on plasma membrane domains of ectodermal epithelia of *Drosophila*. *Cell* **82**, 67-76.

Yarden, Y. and Ullrich, A. (1988) Growth factor receptor tyrosine kinases. *Annu. Rev. Biochem.* **57**, 443-478.